2017 American Control Conference
Sheraton Seattle Hotel
May 24–26, 2017, Seattle, USA

MIMO Identification of Frequency-Domain Unreliability in SEAs

Gray C. Thomas and Luis Sentis

***Abstract*— We investigate the use of frequency domain identification and convex optimization for obtaining robust models of series elastic actuators. This early work focuses on identifying a lower bound on the $\mathcal{H}_\infty$ uncertainty, based on the non-linear behavior of the plant when identified under different conditions. An antagonistic testing apparatus allows the identification of the full two input, two output system. The aim of this work is to find a model which explains all the observed test results, despite physical non-linearity. The approach guarantees that a robust model includes all previously measured behaviors, and thus predicts the stability of never-before-tested controllers. We statistically validate the hypothesis that a single linear model cannot adequately explain the tightly clustered experimental results. And we also develop an optimization problem which finds a lower bound on the $\mathcal{H}_\infty$ uncertainty component of the robust models which we use to represent the plant in all the tested conditions.**

I. Introduction

It is widely acknowledged that robust $\mathcal{H}_\infty$ control theory depends heavily on its assumption of a validated $\mathcal{H}_\infty$ plant model. Without one, the parameters of the uncertainty model revert to another knob the control engineer tweaks to adjust controller performance. But when the highest performance is desired, when the cost of input is negligible, and when the sensitivity is limited by uncertainty alone, we expect this uncertainty model to represent some sort of physical limit to the plant. In this paper we study the physical component of the uncertainty model, which we term *unreliability*, for a series elastic actuator—a fourth order system just complex enough to warrant state-space control. Many open questions in the study of series elastic actuators require a physically-motivated unreliability model for a satisfactory answer, including the question of which output impedances can be attained through feedback control while guaranteeing internal stability.

Perhaps the most well known system identification framework, minimizing the prediction error [1] leads to high quality linear models complete with a measure of model certainty in the form of a model parameter covariance matrix. This parameter covariance, its implication for robust control, and the influence of weighting functions and closed loop identification controllers on it have all been extensively studied. [2], [3], [4], [5] This confidence measure is often taken out of context, however, as it represents only the distribution of models which would result from the same identification process if the data were regenerated. Prediction error uncertainty is not capable of representing phase lag beyond the known model order, nor can it represent the influence of a nonlinearity. [6] Moreover, with additional data the model parameter covariance will decrease even if the error variance is constant—a sought after property of consistency—but a property which clearly indicates that the parameter covariance is not a measure of any physical property.

A paradigm known as stochastic embedding [6], has been proposed to work around this—adding an additional source of uncertainty to the computation of parameter covariance. By supposing that the model parameters are sampled from

This work was supported by NASA Space Technology Research Fellowship grant NNX15AQ33H, "Controlling Robots with a Spring in Their Step," for which Gray is the Fellow and Luis is the Advising Professor. Both authors are with the Department of Mechanical Engineering, University of Texas at Austin, Austin, TX 78712, USA. Send correspondence to gray.c.thomas@utexas.edu

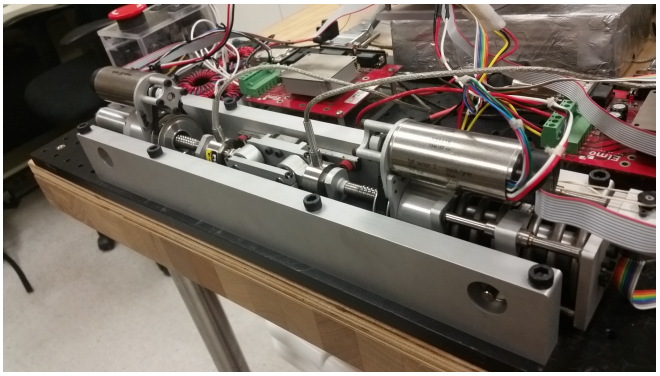

Fig. 1. Antagonistic identification hardware setup. Setup identifies a series elastic ball-screw differential actuator (bottom right) with a second rigid ball-screw differential actuator actuator (top left) to excite an external force.

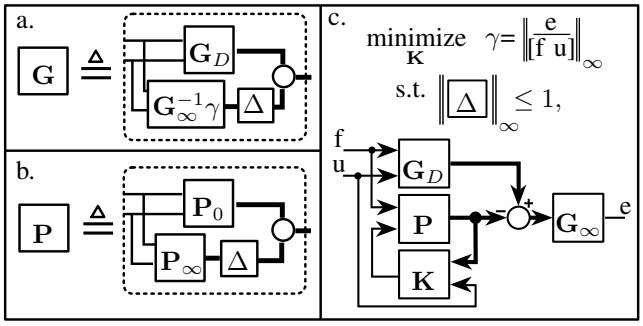

Fig. 2. Components of a "Tower of $\mathcal{H}_\infty$ Guarantees," the long term promise of research in this direction. a.—A description of $\mathcal{H}_\infty$ guaranteed model performance under closed loop control. b.—An $\mathcal{H}_\infty$ model of the series elastic actuator. c.—A model reference control design optimization problem (a structured uncertainty problem) which can build a from b. Since the guaranteed performance has the same form as the initial model the optimization problem can be viewed as a recursive building process, which closes loops to build more complex guarantees. The result is, to put it poetically, a tower of guarantees with system identification as the foundation.

a distribution with pre-defined covariance, the stochastic embedding approach estimates the means of these parameter distributions rather than the parameters themselves—and returns a much more conservative covariance estimate. This covariance doesn't approach zero with more samples—instead it approaches the a-prior covariance. Unfortunately, this means the approach is still heuristic in practice—a justification for padding the covariance estimates from the prediction error method.

The primary alternative to prediction error identification is broad-spectrum frequency-domain estimation. This approach uses a ratio of the Fast Fourier Transform (FFT) spectra of the input to the output. To eliminate noise, the FFT data must be averaged in the frequency domain, often weighted by the magnitude of the input (or occasionally by the magnitude of the output)—making a ratio of cross spectrum to power spectrum. An uncertainty boundary can be obtained by repeatedly generating estimates of the transfer function and then drawing a bound around them numerically [7], but the broad spectrum of the input makes it difficult for this method to capture the full variability of the plant's input–output response, and also understates the transfer function near poles with low damping ratios.

Our identification strategy falls under the broad category of stepped-sine, or "swept sine" in industry [8]. Under this category of approaches the excitation signals carry only a single sinusoidal excitation at a time, and this sinusoid's frequency is then swept through a range in discrete increments. This measures the steady state sinusoid response of the system directly. The sinusoidal component at the tested frequency is often used in place of the real signal, to ignore the harmonic response generated by nonlinearities, and we do this as well.

In an effort to capture a physical component to the $\mathcal{H}_\infty$ robust model, we repeat the tests for each frequency several times, varying the conditions of our experiment several times for each reference signal. These conditions, including the amplitudes and phase lag between the two sinusoidal excitation signals, should not change the estimation of a linear model if our plant were indeed linear. But they do, and we show this empirically, using the classical statistical analysis of variance. We then derive constraints on the transfer matrices of an $\mathcal{H}_\infty$ robust model which is guaranteed to include all observed input output behavior within the robust region of predicted behavior. Our concept of unreliability is closely connected to the far older concept of a describing function [9], but includes factors other than input amplitude and focuses on stability robust to all possible conditions, rather than aiming to predict limit cycles and regions of convergence.

Our long term goal is identification and robust modeling of the NASA R5 Valkyrie [10] robot's actuators for high performance feedback control. We have employed an antagonistic testbed Fig. 1 which tests a differential ball-screw drive UT-SEA [11] that is the predecessor of the differential roller-screw drive SEAs in Valkyrie's chest and ankles. We ultimately aim to improve over the performance of the state of the art disturbance observer based impedance controller,

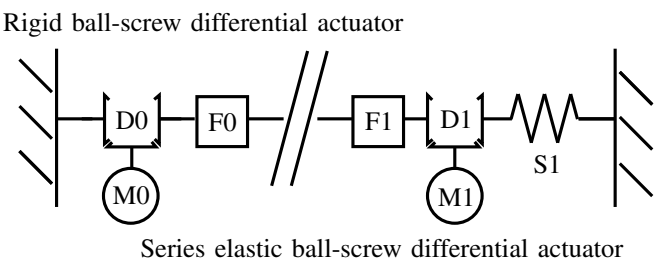

Fig. 3. Schematic for testing configuration. D0 and D1 are ball screw differentials, F0 and F1 are force sensors, M0 and M1 are motors with encoders, and S1 is a spring with a deflection encoder. The input vector to the SEA model is (M1 current, F1 force) and the output is (M1 position, S1 position). However, the system identification software controls the two motor currents and reads all five sensors—and can be configured to perform closed loop identification, which we use in this paper.

[12], by implementing the more general paradigm of model reference control: an $\mathcal{H}_\infty$ design goal similar to [13]. We also seek to incorporate and a robustness requirement similar to [14], but using an $\mathcal{H}_\infty$ frequency-domain uncertainty set informed by the identification system from this paper.

This paper studies the construction of a lower-bound on the $\mathcal{H}_\infty$ uncertainty model which is based on measurable physical properties. Ultimately the $\mathcal{H}_\infty$ uncertainty must include three factors: measurement uncertainty due to noise, intentional simplification due to limited model order, and unreliability under different test conditions—the focus of this paper. As the experiments become more extensive, and as the model approaches the best possible linear description of the real system in the relevant frequency region, this unreliability factor limits the shape of the $\mathcal{H}_\infty$ model. An accurate identification of model unreliability is key to using robust control to reach the physical performance limits of the hardware, quantifying these limits, and understanding the impact of mechanical design decisions from a controls perspective.

II. Frequency Domain Identification Strategy

Modeling a series elastic actuator in the frequency domain, we see it as a collection of transfer functions relating two inputs, current (u_0) and external force (u_1), to two outputs: a motor position encoder (y_0), and a spring deflection encoder (y_1). The four transfer functions between inputs and outputs form a transfer matrix

$$P(j\omega) = \begin{pmatrix} \frac{y_0}{u_0}(j\omega) & \frac{y_0}{u_1}(j\omega) \\ \frac{y_1}{u_0}(j\omega) & \frac{y_1}{u_1}(j\omega) \end{pmatrix}. \tag{1}$$

We use vector notation to express a steady state sinusoidal input signal, output signal, and measurement noise signal

$$y(j\omega), u(j\omega), \eta \in \mathbb{C}^2, \tag{2}$$

often dropping the $j\omega$ function argument when we can infer a particular frequency by context. We assume that the noise is multivariate normal distributed, $\eta \sim \mathcal{N}(0, \Sigma)$, for some Hermitian covariance matrix Σ.

We consider the following two models to be fundamentally different

$$y(j\omega) = P(j\omega)u(j\omega) + \eta, \tag{3}$$

$$y(j\omega) = P(j\omega)u(j\omega) + \Delta J(j\omega)u(j\omega) + \eta \quad \text{s.t.} \quad \Delta^*\Delta \preceq I \tag{4}$$

Where Δ is the local deviation, and Δ^* is its conjugate transpose. $J(j\omega)$ is a weighting transfer matrix, the magnitude of which bounds the model uncertainty—including the unreliability we seek to identify. We term (3) the linear model, and (4) the robust, or $\mathcal{H}_\infty$ model, since the condition on Δ is equivalent to $\|\Delta\|_\infty \leq 1$.

As shown in Fig. 3, the antagonistic SEA testing apparatus has five sensors (M1 position, S1 "force", M0 position, F0 force, and F1 force) and two input motor currents (M1 current, and M0 current). We directly control the two motor current driver commands, and measure the external force acting on the SEA using the F1 force sensor. This is an important improvement over a single input testing protocol because even an indirect second input allows full independence between the motor current and external force inputs.

In order to keep our system away from the hard actuator position limits, we have identified it in closed loop. We implemented two copies of the same PD controller on the two motors, making the input currents

$$\begin{aligned} i_{\mathrm{M1}}(t) =& c_0 + c_1\cos(\omega t) - c_2\sin(\omega t) \\ & - K_p\theta_{\mathrm{M1}}(t) - K_d\dot{\theta}_{\mathrm{M1}}(t) \end{aligned} \tag{5}$$

$$\begin{aligned} i_{\mathrm{M0}}(t) =& c_3 + c_4\cos(\omega t) - c_5\sin(\omega t) \\ & - K_p\theta_{\mathrm{M0}}(t) - K_d\dot{\theta}_{\mathrm{M0}}(t), \end{aligned} \tag{6}$$

where θ_{M0}, and θ_{M1} refer to the two motor encoder positions, the over-dot refers to a time derivative[1]. The parameter vector $(c_0, c_1, c_2, c_3, c_4, c_5)$ defines the experimental conditions we later use to group the data.

We define a *condition group*[2] to be a set of experiments which share the same experimental *conditions*. In our case this means the parameter vector $(c_0, c_1, c_2, c_3, c_4, c_5)$. In general, the choice of condition groups determines the stability guarantee the robust model provides. We assume that the local deviation Δ is constant within a condition group.

A. Single Period Phasor Transform

Frequency domain transfer functions can be thought of as the linear relationship between sinusoidal input signals and sinusoidal output signals in steady state. Sinusoidal signals at a known frequency can be represented by complex phasors. We let phasors be defined by a *Phasor Transform* based on the Fourier transform of a variable[3],

$$\mathcal{F}(f(t)) = \int_{-\infty}^{\infty} f(t)e^{-j\omega t}dt, \tag{7}$$

[1]Actually an estimate obtained using a discrete time implementation of a low pass filter differentiator.

[2]Not to be confused with the algebraic notion of a group

[3]Of course, this is not the only way to arrive at this result.

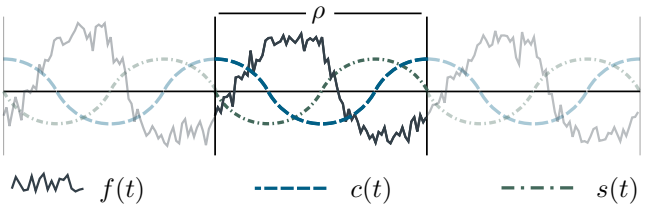

$$c(t) = \omega\cos(\omega t)/\pi, \quad s(t) = -\omega\sin(\omega t)/\pi$$

$$\mathcal{P}_0(f) = \int_0^\rho f(t)c(t)dt + j\int_0^\rho f(t)s(t)dt$$

Fig. 4. Concept illustration for the Single Period Phasor Transform (SPPT) as convolution with scaled sine and cosine signals. This mirrors the hardware implementation.

where the phasor transform is scaled so that purely sinusoidal signals have a finite phasor transform at their frequency, and are otherwise zero:

$$\mathcal{P}(f(t)) = \lim_{T\to\infty} \frac{\int_{-T}^{T} f(t)e^{-j\omega t}dt}{\int_{-T}^{T}\cos(\omega t)e^{-j\omega t}dt} \tag{8}$$

However they are often defined more simply—a phasor is a complex number z which maps to a sinusoidal signal as

$$f(t) = \Re[ze^{j\omega t}] = \Re[z]\cos(\omega t) - \Im[z]\sin(\omega t). \tag{9}$$

Where $\Re$ and $\Im$ select the real and imaginary parts of complex numbers. We note the relationship to the Fourier transform because we use a ratio of phasors to estimate a ratio of Fourier transforms. Moreover, we split up the calculation of a phasor

$$\mathcal{P}(f(t)) = \lim_{N\to\infty} \frac{\sum_{n=-N}^{N-1} \frac{\omega}{\pi}\int_{n2\pi/\omega}^{(n+1)2\pi/\omega} f(t)e^{-j\omega t}dt}{2N} \tag{10}$$

So that we can justify approximating it with an average of many sequential *Single Period Phasor Transform* results,

$$\mathcal{P}_k(f) = \frac{\omega}{\pi}\int_0^{2\pi/\omega} f(t - 2\pi k)e^{-j\omega t}dt. \tag{11}$$

Our system identification software efficiently records the Single Period Phasor Transform (SPPT) of both input and all five output signals. We then use the four records corresponding to the M1 current, the F1 force sensor, the M1 encoder, and the S1 encoder to find a model of the SEA. The records are split up by frequency, and then the records at the same frequency are split up by the test conditions, forming what we call condition groups. Data is discarded at the beginning of each new test condition, to ignore the transient between steady state behaviors. We index the condition groups with the integer $g \in 1, \ldots, N$, where N is the number of condition groups, and the individual SPPT results with the integer $i \in 1, \ldots, N_g$, where N_g is the number of completed periods after steady state in condition group g.

As previously mentioned, we consider the system to be Multiple-Input, Multiple-Output (MIMO), and vectorize the

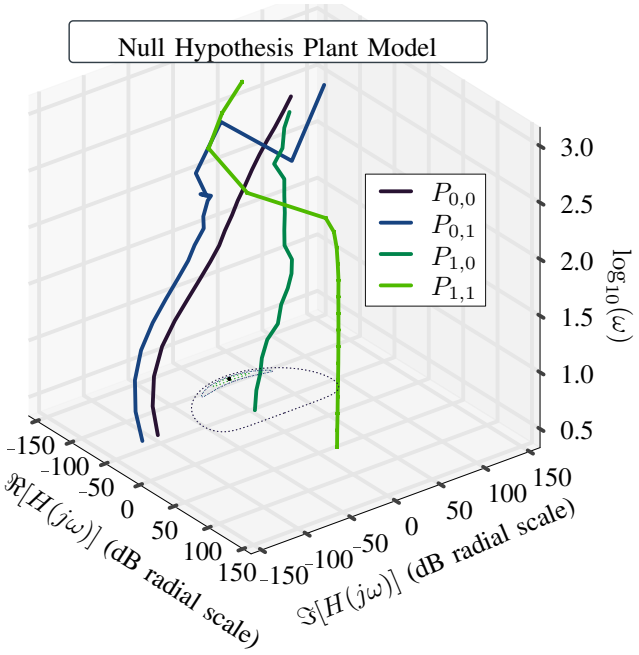

Fig. 5. Best fit linear model for each tested frequency.

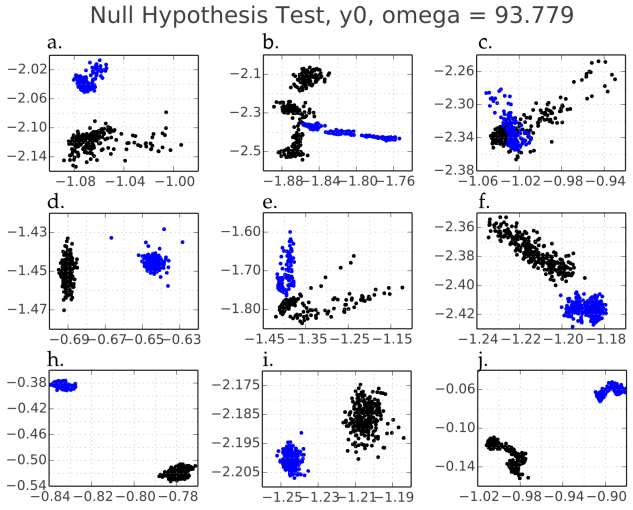

Fig. 6. Output phasors (black) against linear model predictions (blue) for nine randomly generated condition groups plotted a–j. It is hard to visualize the features that are directly tested in the F-test, but this plot shows the tight and distinct clustering of the condition group results relative to the best possible linear model, and the F-test can be said to indirectly test for this. The y_0 variable predicted in these plots is the motor encoder position. It also shows the transients and clustered equilibria that the SPPT allows, see SubFigs. b and e in particular. Without loss of generality, we have assigned the phase of the overall motor translation component of each experiment to be approximately $-135°$ relative to the start of the SPPT clock, and this explains why all nine phasor clusters fall into the third quadrant.

two inputs and two outputs. At angular frequency ω the input vector u refers to a vector of complex numbers, the first element representing the SPPT of the M1 current and the second the SPPT of the F1 force. Adding double subscripts, $u_{g,i}$ specifies the result of the gth condition group, and the ith period of the excitation signal since the start of that condition group's steady state recording period.

III. Statistical Validation of Unreliability

The model (4) treats the physical plant as an uncertain transfer matrix plus noise. The premise of model *unreliability* is that repeating the same test will produce nearly the same result every time, but that different tests will vary much more from a linear model. Essentially, this is saying that the noise term in (4) has a much smaller variance than the noise term in (3). This premise can be supported statistically, using a common technique called analysis of variance, or ANOVA. An ANOVA is traditionally described as a statistically refutation of a null hypothesis—a statistical proof by contradiction. In this case our null hypothesis is that the linear model (3) has produced the data in all the condition groups. Thus the residual,

$$\epsilon_{g,i} = y_{g,i} - P u_{g,i}, \tag{12}$$

for condition group g's ith element, should be samples drawn from a single multivariate distribution. We use least squares to find the transfer matrix P which minimizes the trace of the covariance of η for each angular frequency ω, as shown in Fig. 5. In the data, the residuals for each condition group are almost identical, and many condition groups have average residuals which are far from zero. However, under the null hypothesis, this is exceedingly unlikely. Instead, the null hypothesis claims that while the condition groups will have average residuals which are not quite zero, the average

$$E_g = \sum_{i=1}^{N_g} \epsilon_{g,i}/N_g \in \mathbb{C}^2 \tag{13}$$

of the N_g samples from condition group g should deviate from zero with a covariance matrix about $\frac{1}{N_g}$ times the covariance of the samples themselves. This means that the averages of each condition group can be used to estimate the covariance of the samples as

$$\Sigma_{\text{“group avg.”}} = \frac{\sum_{g=1}^{N} E_g E_g^* N_g}{N-2}. \tag{14}$$

But this can also be estimated using the deviation of the samples within their respective groups from their group average

$$\Sigma_{\text{“within group”}} = \frac{\sum_{g=1}^{N}\sum_{i=1}^{N_g}(\epsilon_{g,i}-E_g)(\epsilon_{g,i}-E_g)^*}{\sum_{g=1}^{N}(N_g-1)}. \tag{15}$$

Let us define the following distance metric between hermitian matrices

$$\Sigma_1/\Sigma_2 = \operatorname{tr}\left[K^{-1}\Sigma_1 K^{-*}\right]/\operatorname{tr}[I], \quad | \quad KK^* = \Sigma_2. \tag{16}$$

With I the identity matrix of the same size as Σ_1 and Σ_2, so that $\operatorname{tr}[I]$ is just 2 for our matrices in $\mathbb{C}^{2\times 2}$. Note that

such a K exists for all positive definite Hermitian matrices—this is known as the Cholesky decomposition. In essence, this construction uses the Cholesky decomposition of Σ_2 to transform the covariance of Σ_1 into the space of estimated covariances for a standard multivariate Gaussian. Taking the trace of this matrix and then dividing it by the trace of the identity matrix is a construction to find the average eigenvalue.

Following the logic of the null hypothesis, the residuals are normally distributed and we expect the distance between the two sample covariance estimates

$$F = \Sigma_{\text{“group avg.”}} / \Sigma_{\text{“within group”}} \tag{17}$$

to be near one and, more specifically, f-distributed with $4(N-2)$ and $4\sum_{g=1}^{N}(N_g - 1)$ degrees of freedom. The factor of four accounts for the use of complex numbers, and the use of two dimensional vectors. We validated this with a simple Monte-Carlo simulation, noting strong similarity between the empirical cumulative distribution function generated by 1000 trials and the cumulative distribution function for the f-distribution.

In statistics there is a concept of a *P-value*, which is defined as the probability of obtaining a result more extreme or equal to the result observed. Statistical hypothesis are refuted by showing that the observed result has an extremely low P-value according to the expected distribution defined in the hypothesis. As is clear from Fig. 7, $F \gg 1$, a result the null hypothesis predicts to be exceedingly unlikely, with a P-value $P \ll 10^{-15}$. From this we can conclude that the condition groups show more variation in their overall behavior than can be explained by the small amount of variation between repeated measurements of the same conditions. In other words, we can expect the condition groups to produce samples which deviate from the linear model in almost the same way every time. It is this repeatable deviation from a linear model which we intend to capture in the notion of unreliability, and which puts a lower limit on the $\mathcal{H}_\infty$ norm of $J(j\omega)$ from (4).

IV. $\mathcal{H}_\infty$ Interpretation of the Results

Given condition groups which represent fundamentally different linear behaviors, we can determine conditions on the transfer matrices in (4) which guarantee that the input output behavior of each condition group is included within the potential behavior of the model.

For simplicity, we first consider the single-input single-output (SISO) case, where each condition group can provide an estimate of the transfer function directly, via phasor division. For each frequency tested and for each condition group tested at that frequency, we have an average input phasor u and an average output phasor y. The ratio y/u provides a point in the complex plane representing an estimate of the observed behavior of the transfer function. Considering all the condition groups tested at that frequency, we can plot a cluster of observed behaviors. If we draw a circle around all the estimates we can interpret that circle as an $\mathcal{H}_\infty$ model of

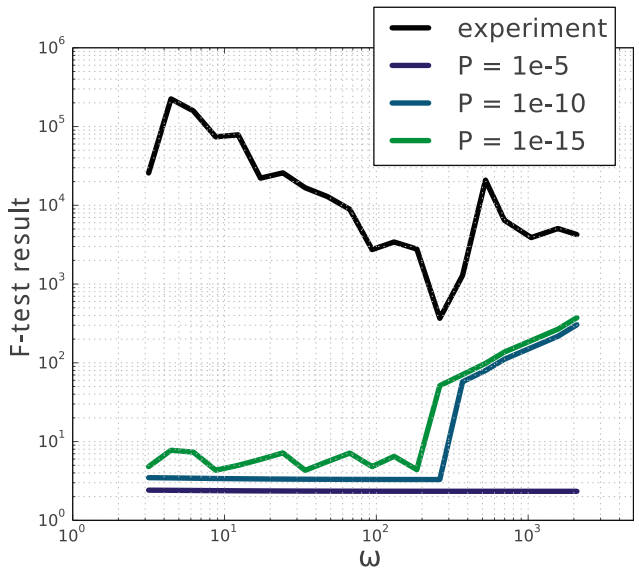

Fig. 7. Statistical significance of group deviation from best possible linear fit at each frequency, using ANOVA for complex vector data. Different frequencies have different numbers of experiments, hence the critical F-test values for different P-values are shown for comparison. There may be numerical accuracy issues at play in computing the cutoff values for such small p-values, however it is clear that the astronomically high F-test values are statistically significant.

the transfer function evaluated at that frequency. The smallest possible radius, r of such a circle is thus a lower bound on the $\mathcal{H}_\infty$ uncertainty—which will ultimately also include factors representing estimation uncertainty due to noise, and under-modeling. This intuition informs the following condition imposed on a MIMO model.

Each condition group has a single input signal, and this means that only a linear projection of the MIMO model can be identified for each condition group. We can use the singular value constraint on Δ,

$$I - \Delta^*\Delta \succeq 0, \tag{18}$$

to relate the measurement to the possible values of P and J at ω. We do this by pre-multiplying by u^*J^* and post multiplying by Ju,

$$u^*J^*Ju - u^*J^*\Delta^*\Delta Ju \geq 0, \tag{19}$$

Which results in a one dimensional real inequality. We can replace a term using (4),

$$\Delta Ju = Pu + \eta - y. \tag{20}$$

However, this estimate is corrupted by the noise η, and the way we choose to deal with the noise will determine the conservatism of the bound. For now, we will simply average the phasor vectors within the condition groups and assume that the noise in the average, which now has covariance Σ/N_g, can be ignored. After replacement,

$$u^*J^*Ju - (Pu - y)^*(Pu - y) \geq 0, \tag{21}$$

which expands,

$$u^*(J^*J - P^*P)u + 2u^*P^*y \geq y^*y. \tag{22}$$

Seeking a linear inequality for computationally efficient optimization, we introduce

$$Q \triangleq J^*J - P^*P, \tag{23}$$

which is Hermitian by construction. We can use the Kronecker product, $\otimes$, and the vectorization operator, vec, to express

$$(u^T \otimes u^*)\mathrm{vec}(Q) + 2(y^T \otimes u^*)\mathrm{vec}(P^*) \geq y^*y \tag{24}$$

Note that when re-constructing J from Q and P there will be ambiguity up to a unitary transform. This is unsurprising, since the Δ model uncertainty objects are permitted to include such transforms. Note as well that this means the uncertainty model is incapable of representing larger uncertainty in one output than another.

In the SISO case there is an obvious choice for an optimization criteria: to minimize the absolute value of the scalar J, equivalent to the geometric radius of the $\mathcal{H}_\infty$ circle in the complex plane. However in the MIMO case there is more ambiguity, since a hyper ellipsoid is being fit to contain a bunch of points and there are many ways to define optimum in this case. We can optimize the trace to arrive at a linearly constrained quadratic optimization problem

$$\begin{aligned} \min_{Q,G\in\mathbb{C}^{2\times 2}} \quad & \mathrm{tr}(Q + P^*P) \\ s.t. \quad & Q = Q^*, \\ & (u_g^T \otimes u_g^*)\mathrm{vec}(Q) \\ & + 2(y_g^T \otimes u_g^*)\mathrm{vec}(P^*) \\ & \geq y_g^*y_g \ \ \forall\ g = 1, \ldots, N \end{aligned}$$

V. Discussion

This final form of the optimization problem is convex, having a quadratic cost and linear inequality constraints. And this is the ultimate result of this study: the unreliability of our plant has been convincingly shown to exist, has been measured, and defines a computationally tractable limit on robust models. In the future we hope to expand on this result by generating a finite dimensional model which satisfies the optimization constraints. We also aim to apply state-of-the-art structured $\mathcal{H}_\infty$ synthesis techniques to build actuator controllers with guaranteed performance out of robust plant models, as suggested in Fig. 2. From there we hope to keep building upwards, using robust actuator controllers to design whole body robot controllers with frequency domain performance guarantees, ultimately allowing us to answer questions about the input–output capabilities of the robot—e.g. the robot's ability to stabilize inverted pendulum behaviors, or the haptic rendering quality of the robot's human interactions.

Clearly, system identification can hardly be expected to construct models which are robust to unmeasured factors or untested conditions. Unmeasured factors cause deviations which are hardly distinct from noise. If amplitudes within a certain range are used to construct a robust model, then a robust controller for that model may still become unstable outside of that amplitude range. It ultimately remains the responsibility of the control engineer to understand the important aspects of the plant and ensure that they are represented in the test. We hope that our statistical analysis can be extended to answer questions in this domain as well, determining if additional factors merit inclusion in the condition vector.

References

[1] L. Ljung, Ed., *System Identification (2Nd Ed.): Theory for the User*. Upper Saddle River, NJ, USA: Prentice Hall PTR, 1999.

[2] Z. Zang, R. R. Bitmead, and M. Gevers, "Iterative weighted least-squares identification and weighted lqg control design," *Automatica*, vol. 31, no. 11, pp. 1577–1594, 1995.

[3] U. Forssell and L. Ljung, "Closed-loop identification revisited," *Automatica*, vol. 35, no. 7, pp. 1215–1241, 1999.

[4] P. Albertos and A. Sala, *Iterative identification and control: advances in theory and applications*. Springer, 2002.

[5] X. Bombois, M. Gevers, G. Scorletti, and B. D. Anderson, "Robustness analysis tools for an uncertainty set obtained by prediction error identification," *Automatica*, vol. 37, no. 10, pp. 1629–1636, 2001.

[6] S. Tøffner-Clausen, *System identification and robust control: A case study approach*. Springer, 1996.

[7] K. Zhou and J. C. Doyle, *Essentials of robust control*. Prentice hall Upper Saddle River, NJ, 1998.

[8] D. Y. Abramovitch, "Trying to keep it real: 25 years of trying to get the stuff i learned in grad school to work on mechatronic systems," in *2015 IEEE Conference on Control Applications (CCA)*. IEEE, 2015, pp. 223–250.

[9] R. J. Kochenburger, "A frequency response method for analyzing and synthesizing contactor servomechanisms," *Transactions of the American Institute of Electrical Engineers*, vol. 69, no. 1, pp. 270–284, 1950.

[10] N. A. Radford, P. Strawser, K. Hambuchen, J. S. Mehling, W. K. Verdeyen, A. S. Donnan, J. Holley, J. Sanchez, V. Nguyen, L. Bridgwater *et al.*, "Valkyrie: Nasa's first bipedal humanoid robot," *Journal of Field Robotics*, vol. 32, no. 3, pp. 397–419, 2015.

[11] N. Paine, S. Oh, and L. Sentis, "Design and control considerations for high-performance series elastic actuators," *IEEE/ASME Transactions on Mechatronics*, vol. 19, no. 3, pp. 1080–1091, 2014.

[12] J. S. Mehling, J. Holley, and M. K. O'Malley, "Leveraging disturbance observer based torque control for improved impedance rendering with series elastic actuators," in *Intelligent Robots and Systems (IROS), 2015 IEEE/RSJ International Conference on*. IEEE, 2015, pp. 1646–1651.

[13] J. S. Mehling and M. K. O'Malley, "A model matching framework for the synthesis of series elastic actuator impedance control," in *Control and Automation (MED), 2014 22nd Mediterranean Conference of*. IEEE, 2014, pp. 249–254.

[14] K. Haninger, J. Lu, and M. Tomizuka, "Robust impedance control with applications to a series-elastic actuated system," in *Intelligent Robots and Systems (IROS), 2016 IEEE/RSJ International Conference on*. IEEE, 2016, pp. 5367–5372.